

N75-13319

CR-132641

FRACTURE OF COMPOSITE PLATES
CONTAINING PERIODIC BUFFER STRIPS

by

F. ERDOGAN and M. BAKIOGLU



October 1974
Lehigh University
Bethlehem, Pennsylvania

THE NATIONAL AERONAUTICS AND SPACE
ADMINISTRATION GRANT NGR 39-007-011

FRACTURE OF COMPOSITE PLATES CONTAINING PERIODIC BUFFER STRIPS*

by

F. Erdogan and M. Bakioglu
Lehigh University, Bethlehem, Pa. 18015

Abstract

In this paper the fracture problem of a composite plate which consists of perfectly bonded parallel load carrying laminates and buffer strips is considered. It is assumed that the fatigue cracks may appear and spread in main laminates or in buffer strips or in both perpendicular to the interfaces. The external load is applied to the plate parallel to the strips and away from the crack region. The problem is solved for fully imbedded cracks and for broken laminates or strips and the corresponding stress intensity factors are calculated.

1. INTRODUCTION

In designing with high strength composite sheet materials the use of relatively low stiffness and high toughness buffer strips oriented parallel to the main load-carrying laminates has been under investigation for some time. The practical aim of this particular design practice is to improve the fatigue crack propagation and arrest characteristics of the structure. The fracture process may start as the initiation of a fatigue crack at a local imperfection in the load carrying laminate. The cyclic history of the applied loads permitting, it may then be possible for the crack to enter the adjacent buffer strips as a result of subcritical or critical growth. Fatigue cracks may also appear and propagate in the buffer strips. Knowing the fatigue and fracture characteristics of both materials, for studies relating to life and structural integrity it would therefore be necessary to have

*This work was supported by the National Aeronautics and Space Administration under the Grant NGR 39-007-011 and by the National Science Foundation under the Grant GK-42771X.

a reliable analysis of the problem. Particularly in fatigue crack propagation studies it would be very helpful to have a technique for the calculation of corresponding stress intensity factors.

Even though in actual structures the primary laminates and the buffer strips would be anisotropic, in this study, largely for reasons of analytical expediency, it will be assumed that both materials are isotropic and linearly elastic. The laminates and the buffer strips containing cracks of arbitrary length perpendicular to the interfaces are assumed to be perfectly bonded and periodically arranged (Figure 1). The composite plate is loaded parallel to the interfaces away from the crack region. The case in which the propagating crack terminates at a bimaterial interface is separately studied. For various crack geometries and for a certain material combination the stress intensity factors are calculated. In recent years the solutions of various special cases of this problem have appeared in literature. Referring to Figure 1, for example, the case of a single strip, (i.e., $\mu_2 = 0$) is investigated in [1] and [2], the problem of two half planes bonded through a cracked strip (i.e., $h_2 = \infty$, $b = 0$, $a < h_1$) is studied in [3] and [4], the solution to the same problem with the broken laminate (i.e., $h_2 = \infty$, $b = 0$, $a = h_1$) may be found in [5]. The problem of two bonded half planes with the finite cracks terminating at or going through the interface was considered in [6] and [7].

2. FORMULATION OF THE PROBLEM

Consider the elastostatic problem for the two-dimensional composite medium shown in Figure 1. It is assumed that two sets of periodically arranged laminates or strips of finite widths $2h_1$ and $2h_2$ are perfectly bonded along their straight boundaries. The strips 1 and 2 are assumed to contain symmetrically located cracks of lengths $2a$ and $2b$, respectively and to have the respective elastic constants μ_1, κ_1 and μ_2, κ_2 where $\kappa_j = 3 - 4\nu_j$ for plane strain and $\kappa_j = (3 - \nu_j)/(1 + \nu_j)$ for generalized plane stress, ν_j , ($j = 1, 2$) being the Poisson's ratio. The external loads are assumed to be such that the periodic nature of the problem is preserved and the crack plane is a plane of symmetry. The solution of the actual traction-free crack problem may be obtained by means of the usual superposition technique. In this paper we will therefore consider the singular part of the problem in which the self-equilibrating crack surface tractions are the only external loads. Thus, referring to Figure 1, the solution of the problem may be obtained by solving the related field equations for the two strips under the following boundary and continuity conditions:

$$u_1(0, y) = u_2(0, y), \quad v_1(0, y) = v_2(0, y), \quad (0 \leq y < \infty), \quad (1.a, b)$$

$$\sigma_{1xx}(0, y) = \sigma_{2xx}(0, y), \quad \sigma_{1xy}(0, y) = \sigma_{2xy}(0, y), \quad (0 \leq y < \infty), \quad (2.a, b)$$

$$u_1(-h_1, y) = 0, \quad \sigma_{1xy}(-h_1, y) = 0, \quad (0 < y < \infty), \quad (3.a, b)$$

$$u_2(h_2, y) = 0, \quad \sigma_{2xy}(h_2, y) = 0, \quad (0 < y < \infty), \quad (4.a, b)$$

$$\sigma_{1xy}(x, 0) = 0, \quad (-h_1 \leq x < 0), \quad \sigma_{2xy}(x, 0) = 0, \quad (0 < x \leq h_2), \quad (5.a, b)$$

$$\sigma_{1yy}(x, 0) = -p_1(x), \quad (-h_1 \leq x < a - h_1), \quad v_1(x, 0) = 0, \quad (a - h_1 < x < 0), \quad (6.a, b)$$

$$\sigma_{2yy}(x,0) = -p_2(x), (h_2-b < x < h_2), v_2(x,0) = 0, \\ (0 < x < h_2-b), \quad (7.a,b)$$

$$\sigma_{kyy}(x,\infty) = 0, \sigma_{kxy}(x,\infty) = 0, (k=1,2), \quad (8)$$

where, because of symmetry, only one quarter of a strip from each set is considered. In (1-8) u_k and v_k are the x and y -components of the displacement vector in the strip k , ($k=1,2$), σ_{kij} , ($k=1,2$, (i,j) = (x,y)) are the usual stress components and p_1 and p_2 are known functions. Defining the coordinates

$$x_1 = x + h_1, x_2 = x - h_2, y_1 = y = y_2, \quad (9)$$

the solution of the problem satisfying the necessary field equations and the conditions (3), (4), (5), and (8) may be expressed as

$$u_i(x_i, y) = -\frac{2}{\pi} \int_0^\infty \left\{ \frac{1}{s} [f_i(s) - \frac{\kappa_i - 1}{2} g_i(s)] \sinh(x_i s) \right. \\ \left. + x_i g_i(s) \cosh(x_i s) \right\} \cos(ys) ds \\ - \frac{2}{\pi} \int_0^\infty m_i(r) r^{-1} \left(\frac{\kappa_i - 1}{2} - ry \right) e^{-ry} \sin(x_i, r) dr, \\ v_i(x_i, y) = \frac{2}{\pi} \int_0^\infty \left\{ \frac{1}{s} [f_i(s) + \frac{\kappa_i + 1}{2} g_i(s)] \cosh(x_i s) \right. \\ \left. + x_i g_i(s) \sinh(x_i s) \right\} \sin(ys) ds \\ + \frac{2}{\pi} \int_0^\infty m_i(r) r^{-1} \left(\frac{\kappa_i + 1}{2} + yr \right) e^{-yr} \cos(x_i, r) dr, \\ (i = 1,2) \quad (10.a,b)$$

where f_i , g_i , and m_i , ($i = 1,2$) are unknown functions which may be determined from the remaining six boundary conditions given by (1), (2), (6), and (7). From (10) the stress components may be obtained

as

$$\frac{1}{2\mu_i} \sigma_{ixx}(x_i, y) = -\frac{2}{\pi} \int_0^\infty [f_i(s) \cosh(x_i s) + s x_i g_i(s) \sinh(x_i s)] * \cos(ys) ds - \frac{2}{\pi} \int_0^\infty m_i(r) (1-yr) e^{-yr} \cos(x_i r) dr,$$

$$* \cos(ys) ds - \frac{2}{\pi} \int_0^\infty m_i(r) (1-yr) e^{-yr} \cos(x_i r) dr,$$

$$\frac{1}{2\mu_i} \sigma_{iyy}(x_i, y) = \frac{2}{\pi} \int_0^\infty \{ [f_i(s) + 2g_i(s)] \cosh(x_i s) + s x_i g_i(s) \sinh(x_i s) \} \cos(ys) ds$$

$$+ s x_i g_i(s) \sinh(x_i s) \} \cos(ys) ds$$

$$- \frac{2}{\pi} \int_0^\infty m_i(r) (1+yr) e^{-yr} \cos(x_i r) dr,$$

$$\frac{1}{2\mu_i} \sigma_{ixy}(x_i, y) = \frac{2}{\pi} \int_0^\infty \{ [f_i(s) + g_i(s)] \sinh(x_i s) + s x_i g_i(s) \cosh(x_i s) \} \sin(ys) ds$$

$$+ s x_i g_i(s) \cosh(x_i s) \} \sin(ys) ds$$

$$- \frac{2}{\pi} \int_0^\infty y r m_i(r) e^{-yr} \sin(x_i r) dr,$$

$$(i = 1, 2).$$

$$(11.a-c)$$

If we now substitute from (10) and (11) into the four continuity conditions (1) and (2) and take the inverse transforms in the variable s , we obtain four algebraic equations for the functions f_1 , g_1 , f_2 , and g_2 . Solving these equations, f_i and g_i , ($i = 1, 2$) may be expressed in terms of $m_1(r)$ and $m_2(r)$. The remaining two mixed boundary conditions would then give a system of dual integral equations for m_1 and m_2 . Appendix A gives the expressions for f_i and g_i , ($i = 1, 2$). Rather than deriving the system of dual integral equations, in this paper the mixed boundary conditions are directly reduced to a system of singular integral equations. Before doing this we observe that the conditions (6.b) and (7.b) are equivalent

to

$$\frac{\partial}{\partial x_i} v_i(x_i, 0) = 0, \quad (a_i < |x_i| < h_i), \quad \int_{-a_i}^{a_i} \frac{\partial}{\partial x_i} v_i(x_i, 0) dx_i = 0,$$

$$(i = 1, 2; a_1 = a, a_2 = b) \quad (12.a, b)$$

If we now define

$$G_i(x_i) = \frac{\partial}{\partial x_i} v_i(x_i, 0), \quad (i = 1, 2), \quad (13)$$

from (12.a) and (10.b) it is seen that

$$m_i(r) = - \frac{2}{\kappa_i + 1} \int_0^{a_i} G_i(t) \sin rt \, dt, \quad (a_1 = a, a_2 = b, \\ i = 1, 2) \quad (14)$$

Thus, substituting from (14), (A1), (A2), and (11.b) into (6.a) and (7.a) we obtain a pair of integral equations for the new unknown functions G_1 and G_2 . With m_i as defined in (14) for $y \rightarrow +0$ the second integral in (11.b) becomes

$$\lim_{y \rightarrow +0} \left[- \frac{2}{\pi} \int_0^\infty m_i(r) (1 + yr) e^{-yr} \cos(x_i r) dr \right] \\ = \frac{2}{\pi(\kappa_i + 1)} \int_0^{a_i} \left(\frac{1}{t - x_i} + \frac{1}{t + x_i} \right) G_i(t) dt, \quad (i = 1, 2). \quad (15)$$

Similarly, the functions defined by (A.1) may be expressed as

$$F_{ij}(s) = \frac{1}{\kappa_i + 1} \int_0^{a_i} [M_{ij}(s, t) - M_{ij}(s, -t)] G_i(t) dt, \\ (i = 1, 2; j = 1, \dots, 4) \quad (16)$$

where

$$\begin{aligned}
M_{i1}(s,t) &= - [s(h_i-t) + \frac{\kappa_i-1}{2}] e^{-s(h_i-t)}, \\
M_{i2}(s,t) &= [s(h_i-t) - \frac{\kappa_i+1}{2}] e^{-s(h_i-t)}, \\
M_{i3}(s,t) &= s(h_i-t) e^{-s(h_i-t)}, \\
M_{i4}(s,t) &= [s(h_i-t) - 1] e^{-s(h_i-t)}, \quad (i = 1,2): \quad (17)
\end{aligned}$$

If we substitute from (15), (16), (A2), and (11.b) into (6.a) and (7.a) and note that because of symmetry

$$G_i(x_i) = -G_i(-x_i), \quad (i = 1,2; -a_i < x_i < a_i) \quad (18)$$

we obtain

$$\begin{aligned}
&\int_{-a}^a \frac{G_1(t)}{t-x} dt + \int_{-a}^a k_{11}(x_1,t) G_1(t) dt + \int_{-b}^b k_{12}(x_1,t) G_2(t) dt \\
&\quad = - \frac{\pi(1+\kappa_1)}{4\mu_1} p_1(x_1-h_1), \quad (-a < x_1 < a), \\
&\int_{-b}^b \frac{G_2(t)}{t-x_2} dt + \int_{-a}^a k_{21}(x_2,t) G_1(t) dt + \int_{-b}^b k_{22}(x_2,t) G_2(t) dt \\
&\quad = - \frac{\pi(1+\kappa_2)}{4\mu_2} p_2(x_2+h_2), \quad (-b < x_2 < b) \quad (19,a,b)
\end{aligned}$$

where the kernels $k_{ij}(x_i,t)$, $(i,j = 1,2)$ are given by

$$k_{ij}(x_i,t) = \int_0^\infty K_{ij}(x_i,t,s) e^{-s(h_i-t)} ds. \quad (20)$$

The expressions for the functions K_{ij} may be found in Appendix B. The index of the system of singular integral equations (19) is +1;

therefore the solution will contain two arbitrary constants [8]. Theoretically these constants are determined by using the single-valuedness conditions (12.b). However, due to symmetry, if one only considers solutions satisfying (18), (12.b) will be automatically satisfied. For $a < h_1$ and $b < h_2$ (Figure -1) from Appendix B it may be shown that the kernels $k_{ij}(x_i, t)$, ($i, j = 1, 2$) are bounded and continuous in the corresponding closed intervals. Thus, in this case, (19) is a system of ordinary singular integral equations with fundamental functions

$$w_1(t) = (a^2 - t^2)^{-\frac{1}{2}}, w_2(t) = (b^2 - t^2)^{-\frac{1}{2}} \quad (21.a, b)$$

and may be solved in a straightforward manner.

All the known special cases may be recovered from (19) by letting the length parameters a , h_1 , b , and h_2 go to proper limits. For example, for $h_1 \rightarrow \infty$ and $h_2 \rightarrow \infty$ k_{ij} vanish, (19) uncouples giving the integral equations for center-notched infinite plates. For $b = 0$, $h_2 \rightarrow \infty$, (19) reduces to an integral equation in $G_1(t)$, the Cauchy kernel and k_{11} being the only kernels. From Appendix B, the integrand giving k_{11} may be shown to reduce to

$$\begin{aligned} K_{11}(x_1, t, s) = & (1 - 4\alpha_1 h_1 s e^{-2h_1 s} - \alpha_1 \alpha_2 e^{-4h_1 s})^{-1} e^{-h_1 s} * \\ & * \{ \alpha_1 \cosh(x, s) [1 - \alpha_2 (3 + 2h_1 s) e^{-2h_1 s}] \\ & - 2x_1 s \alpha_1 \alpha_2 \sinh(x, s) e^{-2h_1 s} + \alpha_2 [1 - 2s(h_1 - t)] * \\ & * [\cosh(x, s) (3 - 2h_1 s - \alpha_1 e^{-2h_1 s}) + 2x_1 s \sinh(x_1 s)] \}. \end{aligned} \quad (22)$$

where the constants α_1 and α_2 are defined in Appendix B.

This is the kernel found in [5]. If $\mu_2 = 0$ (18) further reduces to the kernel obtained for the center-notched strip in [2]. One may also observe that the kernels k_{ij} have the expected property of interchangability in the sense that k_{2j} may be obtained from k_{1j} by changing the necessary indices and letting $\alpha_1 \rightarrow \alpha_3$ and $\alpha_2 \rightarrow \alpha_4$.

3. THE LIMITING CASE: BROKEN LAMINATES.

In the limiting case of broken laminates, (i.e., $a = h_1$ or $b = h_2$) the integral equations (19) are still valid. However, in this case the kernels k_{ij} , ($i, j = 1, 2$) will not all be bounded in the corresponding closed intervals. For example if $a = h_1$, $b < h_2$, examining the integrands $K_{ij}(x_i, t, s)$ given in Appendix B it may be seen that the kernels k_{12} , k_{21} , and k_{22} are bounded for all values of x_1 , x_2 , and t , but k_{11} becomes unbounded as x_1 and t approach the end points $\pm h_1$ simultaneously. The important consequence of this is that for $a = h_1$ (19) is no longer a system of ordinary singular integral equations, it has generalized Cauchy kernels, the fundamental matrix of the system is different than that given by (21), and the solution requires more care. Noting that since K_{11} is bounded and continuous everywhere in $0 \leq s < \infty$, referring to (20) any divergence in the integral must be due to the behavior of the integrand for $s \rightarrow \infty$. Thus separating the asymptotic part K_{11s} of the integrand K_{11} we find

$$K_{11}(x_1, t, s) = K_{11s}(x_1, t, s) + K_{11f}(x_1, t, s),$$

$$k_{11}(x_1, t) = k_{11s}(x_1, t) + k_{11f}(x_1, t),$$

$$k_{11s}(x_1, t) = \int_0^\infty K_{11s}(x_1, t, s) e^{-s(h_1-t)} ds,$$

$$k_{11f}(x_1, t) = \int_0^\infty K_{11f}(x_1, t, s) e^{-s(h_1-t)} ds,$$

$$K_{11s}(x_1, t, s) = e^{-h_1 s} \{ \alpha_1 \cosh(x_1 s) + \alpha_2 [1 - 2s(h_1 - t)] [(3 - 2h_1) s \cosh(x_1 s) + 2s x_1 \sinh(x_1 h)] \},$$

$$(-h_1 < (x_1, t) < h_1), \quad (23.a-e)$$

where k_{11f} is bounded in $-h_1 \leq (x_1, t) \leq h_1$. The singular part of the kernel k_{11s} may be evaluated by using the following result [10]:

$$\begin{aligned} \int_0^\infty s^n e^{-s(2h_1-t)} \left\{ \frac{\sinh(sx_1)}{\cosh(sx_1)} \right\} ds &= \frac{d^n}{dt^n} \int_0^\infty e^{-s(2h_1-t)} \left\{ \frac{\sinh(sx_1)}{\cosh(sx_1)} \right\} ds \\ &= \frac{d^n}{dt^n} \left[\frac{1}{(2h_1-t)^2 - x_1^2} \left\{ \frac{x_1}{2h_1-t} \right\} \right], \quad (n = 1, 2, \dots), \end{aligned} \quad (24)$$

giving

$$\begin{aligned} k_{11s}(x_1, t) &= (\alpha_1 + 3\alpha_2) \frac{2h_1-t}{(2h_1-t)^2 - x_1^2} + \frac{2\alpha_2}{[(2h_1-t)^2 - x_1^2]^2} [x_1^2 t \\ &\quad - (2h_1-t)^2 (4h_1-3t) + [(2h_1-t)^2 - x_1^2]^{-1} \{ 4(h_1 \\ &\quad - t) [(2h_1-t)^2 (2h_1^2 - h_1 t - 3x_1^2) + x_1^2 (6h_1^2 - 3h_1 t - x_1^2)] \}] \\ &= \{ 2\alpha_2 (h_1 + x_1)^2 \frac{d^2}{dx_1^2} + 6\alpha_2 (h_1 + x_1) \frac{d}{dx_1} \\ &\quad - \frac{\alpha_1 - 3\alpha_2}{2} \} [t - (2h_1 + x_1)]^{-1} \end{aligned}$$

$$\begin{aligned}
& + \{2\alpha_2(h_1-x_1)^2 \frac{d^2}{dx_1^2} - 6\alpha_2(h_1-x_1) \frac{d}{dx_1} \\
& - \frac{\alpha_1-3\alpha_2}{2}\} [t-(2h_1-x_1)]^{-1}, \quad (-h_1 \leq (x_1, t) \leq h_1). \quad (25)
\end{aligned}$$

Substituted into (19) and together with $1/(t-x)$, k_{11s} gives a typical generalized Cauchy kernel. In this case the fundamental solution matrix of (19) is of the form

$$w_1(t) = (h_1^2 - t^2)^{-\gamma}, \quad w_2(t) = (b^2 - t^2)^{-\beta}, \quad (0 < \text{Re}(\gamma, \beta) < 1). \quad (26.a, b)$$

The characteristic equations giving the exponents γ and β may be obtained from (19) by letting

$$G_1(t) = H_1(t)(h_1^2 - t^2)^{-\gamma}, \quad G_2(t) = H_2(t)(b^2 - t^2)^{-\beta} \quad (27.a, b)$$

and using the standard complex function technique [8, 2, 5]. In

(27) H_1 and H_2 are assumed to be bounded in the intervals

$-h_1 \leq t \leq h_1$ and $-b \leq t \leq b$, respectively. Omitting the detailed manipulations (see, for example, [2], [5-7]) the characteristic equations are found to be

$$2\cos\pi\gamma + 4\alpha_2(\gamma-1)^2 - (\alpha_1 + \alpha_2) = 0,$$

$$\cos\pi\beta = 0.$$

(28.a, b)

We note that (28.a) is the same as the characteristic equation found in [6] by two different methods for a crack tip terminating at a bimaterial interface and (28.b) gives the known result $\beta = 0.5$. Similar results may be obtained for $b = h_2$, $a < h_1$.

4. THE SOLUTION AND THE RESULTS

For $a < h_1$, $b < h_2$ the system of integral equations (19) has the fundamental functions as given by (21) which are the weights of Chebyshev polynomials. Hence the system may be solved in a straightforward manner by using the Gauss-Chebyshev integration technique described in [9]. For $a = h_1$, $b < h_2$ (or $a < h_1$, $b = h_2$), the fundamental functions of the integral equations are given by (26) where $\beta = 0.5$ and γ is the root of (28.a) for which $0 < \text{Re}(\gamma) < 1$. It may be shown that for all possible material combinations γ is real. In this case the fundamental functions are the weights of Jacobi polynomials and the solution of the integral equations may be obtained by using the Gauss-Jacobi integration technique (see, for example, [5-7]).

After solving (19) from the formulation given in this paper it is clear that all the desired field quantities may be expressed in terms of definite integrals with appropriate Green's functions as kernels and G_1 and G_2 as density functions. In fracture studies one is usually interested only in the stress intensity factors which may be defined in terms of cleavage stresses $\sigma_{iyy}(x_i, 0)$, ($i = 1, 2$) and may be expressed in terms of the derivatives of the crack surface displacements G_1 and G_2 as follows [6]:

$$b < h_2: \quad k_b = \lim_{x_2 \rightarrow b} \sqrt{2(x_2 - b)} \sigma_{2yy}(x_2, 0) = - \frac{4\mu_2}{1+\kappa_2} \lim_{x_2 \rightarrow b} \sqrt{2(b - x_2)} G_2(x_2),$$

$$a < h_1: k_a = \lim_{x \uparrow a} \sqrt{2(x_1 - a)} \sigma_{1yy}(x_1, 0) = - \frac{4\mu_1}{1+\kappa_2} \lim_{x \uparrow a} \sqrt{2(a - x_1)} G_1(x_1),$$

$$a = h_1: k_a = \lim_{x \uparrow h_1} \sqrt{2} (x_2 + h_2)^Y \sigma_{2yy}(x_2, 0) = -2\mu^* \lim_{x \uparrow h_1} \sqrt{2} (h_1 - x_1)^Y \cdot$$

$$\cdot G_1(x_1), \quad (29.a-c)$$

where

$$\mu^* = \frac{\mu_1 \mu_2}{\sin \pi \gamma} \left(\frac{1+2\alpha_1(1-\gamma)}{\mu_1 + \kappa_1 \mu_2} + \frac{1-2\alpha_2(1-\gamma)}{\mu_2 + \kappa_2 \mu_1} \right). \quad (30)$$

As an example we consider the composite medium shown in Figure 1. It is assumed that the problem is one of "plane stress", there is no constraint in x-direction, and the plate is loaded in y-direction sufficiently far away from the crack region. (*) Thus, in the perturbation problem the crack surface tractions are constant and satisfy the following condition:

$$(p_1/p_2) = E_1/E_2 \quad (31)$$

where E_1 and E_2 are the Young's moduli.

Figures 2-5 show some of the calculated results. The material combination used ($\nu_1 = 0.35$, $\nu_2 = 0.45$, $\mu_1 = 6.65\mu_2$) is assumed to approximate boron epoxy sheets having buffer strips

(*) This means that the dimension of the plate in y direction is large compared to that in x-direction. If the opposite is true and if the external load is applied through fixed grips, then in the uncracked plate $\epsilon_y = 0$ and the ratio of the crack surface tractions becomes $(p_1/p_2) = [E_1(1-\nu_2^2)]/[E_2(1-\nu_1^2)]$. In either case the analysis does not apply to the strips on the sides.

of the same material but different stiffness. Figure 2 shows the stress intensity factor k_a for $b = 0$ and varying ratios a/h_1 and h_2/h_1 . Referring to Figure 1, for $a = h_1$ (and $0 \leq b \leq h_2$) the asymptotic value of the cleavage stress around the singular point is (see (29.c))

$$\sigma_{2yy}(x_2, 0) \cong \frac{k_a}{\sqrt{2} (x_2 + h_2)^\gamma}, \quad (x_2 = x - h_2) \quad (31)$$

where, for the materials under consideration $\gamma = 0.7015$. Figure 2 also shows the normalized k_a for $a = h_1$, $b = 0$. As expected for $h_2 \rightarrow 0$ $k_a(a = h_1) \rightarrow \infty$. Note that for $h_2 = 0$ the problem reduces to that of a homogeneous plate with periodic collinear cracks. Figure 3 shows the similar results for $a = 0$, and b/h_2 and h_1/h_2 variable. In this case for $b = h_2$ the stiffness of the adjacent medium is higher and consequently the power of the stress singularity γ becomes less than 0.5 ($\gamma = 0.3621$). The results given in Figures 2 and 3 indicate that the stress intensity factor k_a for a crack in the stiffer material is higher and k_b for a crack in the less stiff material is lower than the stress intensity factor in the corresponding homogeneous plate.

Figures 4 and 5 show the results for the case in which both sets of strips contain cracks. These examples are given for the same material pair as used in Figures 2 and 3, and for a fixed width ratio $h_1/h_2 = 4$. Figure 4 shows the stress intensity factor k_a for various values of a/h_1 and varying b/h_2 . Again for $a = h_1$ the power of the stress singularity γ is greater than 0.5 and the scale for k_a is given on the right with a

normalizing factor $p_1 h_1^\gamma$. Figure 5 shows the stress intensity factor k_b for the same problem. The scale for $k_b/p_2\sqrt{b}$ for the limiting case of $a = h_1$ is shown on the right. Note that for $a = h_1$ $k_b \rightarrow \infty$ as $b \rightarrow h_2$ and for $a < h_1$ k_b tends to zero as $b \rightarrow h_2$. This latter result is due to the change in the power of stress singularity from 0.5 for $b < h_2$ to $\gamma = 0.3621 < 0.5$ for $b = h_2$.

References

1. I.N. Sneddon and R.P. Srivastava, "The stress field in the vicinity of a Griffith crack in a strip of finite width", Int. J. Engng. Sci., Vol. 9, p. 479, (1971).
2. G.D. Gupta and F. Erdogan, "The problem of edge cracks in an infinite strip", J. Appl. Mech., Trans. ASME (to appear, 1975).
3. P.D. Hilton and G.C. Sih, "A laminate composite with a crack normal to the interfaces", Int. J. Solids Structures, Vol. 7, p. 913, (1971).
4. D.B. Bogy, "The plane elastostatic solution for a symmetrically loaded crack in a strip composite", Int. J. Engng. Sci., Vol. 11, p. 985, (1973).
5. G.D. Gupta, "A layered composite with a broken laminate", Int. J. Solids Structures, Vol. 10, p. 1141, (1973).
6. T.S. Cook and F. Erdogan, "Stresses in bonded materials with a crack perpendicular to the interface", Int. J. Engng. Sci., Vol. 10, p. 667, (1972).
7. F. Erdogan and V. Biricikoglu, "Two bonded half planes with a crack going through the interface", Int. J. Engng., Vol. 11, p. 745, (1973).
8. N.I. Muskhelishvili, "Singular Integral Equations", P. Noordhoff, Groningen, Holland, (1953).
9. F. Erdogan and G.D. Gupta, "On the numerical solution of singular integral equations", Quart. Appl. Math., Vol. 30, p. 525, (1972).
10. A. Erdelyi, ed., "Tables of Integral Transforms", Vol. 1, McGraw-Hill, New York, (1953).

APPENDIX A

The expressions for the functions f_i and g_i , ($i = 1, 2$):

The functions f_i and g_i , ($i = 1, 2$) may be expressed in terms of m_1 and m_2 by substituting from (10) and (11) into (1) and (2). First define

$$\begin{aligned} F_{i1}(s) &= \frac{2s}{\pi} \int_0^\infty m_i(r) \left[2s^2 + \frac{\kappa_i - 3}{2} (r^2 + s^2) \right] \frac{\sin(h_i r)}{(r^2 + s^2)^2} dr, \\ F_{i2}(s) &= \frac{2s^2}{\pi} \int_0^\infty m_i(r) \left[2r^2 + \frac{\kappa_i + 1}{2} (r^2 + s^2) \right] \frac{\cos(h_i r)}{r(r^2 + s^2)^2} dr, \\ F_{i3}(s) &= \frac{4s^2}{\pi} \int_0^\infty r m_i(r) \frac{\cos(h_i r)}{(r^2 + s^2)^2} dr, \\ F_{i4}(s) &= \frac{4s}{\pi} \int_0^\infty r^2 m_i(r) \frac{\sin(h_i r)}{(r^2 + s^2)^2} dr, \quad (i = 1, 2). \end{aligned} \quad (A1.a-d)$$

Equations (1) and (2) would then give

$$\begin{aligned} f_i(s) &= \sum_{j=1}^4 (a_{ij} F_{1j} + b_{ij} F_{2j}), \\ g_i(s) &= \sum_{j=1}^4 (c_{ij} F_{1j} + d_{ij} F_{2j}), \quad (i = 1, 2), \end{aligned} \quad (A2.a,b)$$

where

$$\begin{aligned} a_{11}(s) &= [n_1 \cosh(h_2 s) - c_{11} T_1] / S_1, \\ a_{12}(s) &= [n_1 \sinh(h_2 s) - c_{12} T_1] / S_1, \\ a_{13}(s) &= [-\lambda_1 n_2 \sinh(h_2 s) - c_{13} T_1] / S_1, \\ a_{14}(s) &= [\lambda_1 n_2 \cosh(h_2 s) - c_{14} T_1] / S_1, \end{aligned}$$

$$\begin{aligned}
b_{11}(s) &= a_{11}(s), \quad b_{12}(s) = [-n_1 \sinh(h_2 s) - d_{12} T_1] / S_1, \\
b_{13}(s) &= [n_2 \sinh(h_2 s) - d_{13} T_1] / S_1, \\
b_{14}(s) &= [n_2 \cosh(h_2 s) - d_{14} T_1] / S_1, \\
a_{21}(s) &= [n_3 \cosh(h_1 s) - c_{21} T_2] / S_2, \\
a_{22}(s) &= [-n_3 \sinh(h_1 s) - c_{22} T_2] / S_2, \\
a_{23}(s) &= [n_4 \sinh(h_1 s) - c_{13} T_2] / S_2, \\
a_{24}(s) &= [n_4 \cosh(h_1 s) - c_{24} T_2] / S_2, \\
b_{21}(s) &= a_{21}(s), \quad b_{22}(s) = [n_3 \sinh(h_1 s) - d_{22} T_2] / S_2, \\
b_{23}(s) &= [-\lambda_2 n_4 \sinh(h_1 s) - d_{23} T_2] / S_2, \\
b_{24}(s) &= [\lambda_2 n_4 \cosh(h_1 s) - d_{24} T_2] / S_2, \tag{A.3}
\end{aligned}$$

where

$$\begin{aligned}
\lambda_1 &= \mu_1 / \mu_2, \quad \lambda_2 = \mu_2 / \mu_1, \\
S_1 &= [(\lambda_1 - 1)h_2 s - \frac{\lambda_1 \kappa_2 + 1}{2} \sinh(2h_2 s)] \sinh(h_1 + h_2)s, \\
S_2 &= [(\lambda_2 - 1)h_1 s - \frac{\lambda_2 \kappa_1 + 1}{2} \sinh(2h_1 s)] \sinh(h_1 + h_2)s, \\
T_1 &= [(\lambda_1 - 1)h_2 s - \frac{\lambda_1 \kappa_2 + 1}{2} \sinh(2h_2 s)] [h_1 s \cosh(h_1 + h_2)s \\
&\quad + \frac{1}{2} \sinh(h_1 + h_2)s] + [-\frac{\lambda_1 \kappa_2 - \kappa_1}{2} \sinh(2h_2 s) \\
&\quad - (\lambda_1 + \kappa_1)h_2 s] \frac{1}{2} \sinh(h_2 - h_1)s, \\
T_2 &= [(\lambda_2 - 1)h_1 s - \frac{\lambda_2 \kappa_1 + 1}{2} \sinh(2h_1 s)] [h_2 s \cosh(h_1 + h_2)s
\end{aligned}$$

$$\begin{aligned}
& + \frac{1}{2} \sinh(h_1 + h_2)s] + \frac{1}{2} \sinh(h_1 - h_2)s [-(\lambda_2 + \kappa_2)h_1s \\
& + \frac{\lambda_1 \kappa_1 - \kappa_2}{2} \sinh(2h_1s)]. \quad (A.4)
\end{aligned}$$

$$\begin{aligned}
c_{11}(s) &= L_1 \cosh(h_2s) + L_3 \cosh(h_1s), \\
c_{12}(s) &= L_1 \sinh(h_2s) - L_3 \sinh(h_1s), \\
c_{13}(s) &= -L_1 \sinh(h_2s) + \lambda_1 L_3 \sinh(h_1s), \\
c_{14}(s) &= L_1 \cosh(h_2s) + \lambda_1 L_3 \cosh(h_1s), \\
d_{11}(s) &= c_{11}(s), \quad d_{12}(s) = -c_{12}(s), \quad d_{13}(s) = \lambda_2 L_1 \sinh(h_2s) \\
&\quad - L_3 \sinh(h_1s), \\
d_{14}(s) &= \lambda_2 L_1 \cosh(h_2s) + L_3 \cosh(h_1s), \\
c_{21}(s) &= L_2 \cosh(h_1s) + L_4 \cosh(h_2s), \\
c_{22}(s) &= -L_2 \sinh(h_1s) + L_4 \sinh(h_2s), \\
c_{23}(s) &= \lambda_1 L_2 \sinh(h_1s) - L_4 \sinh(h_2s), \\
c_{24}(s) &= \lambda_1 L_2 \cosh(h_1s) + L_4 \cosh(h_2s), \\
d_{21}(s) &= c_{21}(s), \quad d_{22}(s) = -c_{22}(s), \quad d_{23}(s) = -L_2 \sinh(h_1s) \\
&\quad + \lambda_2 L_4 \sinh(h_2s) \\
d_{24}(s) &= L_2 \cosh(h_1s) + \lambda_2 L_4 \cosh(h_2s), \quad (A.5)
\end{aligned}$$

where

$$L_1 = \frac{1}{D} \frac{\kappa_2 + 1}{2} \sinh(h_2 - h_1)s, \quad L_2 = \frac{1}{D} \frac{\kappa_1 + 1}{2} \sinh(h_1 - h_2)s,$$

$$L_3 = \frac{1}{D} [(1-\lambda_2)h_2s - \frac{1}{2}(\lambda_2+\kappa_2)\sinh(2h_2s)],$$

$$L_4 = \frac{1}{D} [(1-\lambda_1)h_1s - \frac{1}{2}(\lambda_1+\kappa_1)\sinh(2h_1s)],$$

$$D = - \frac{(\kappa_1+1)(\kappa_2+1)}{4} \sinh^2(h_1-h_2)s - [(1-\lambda_1)h_2s - \frac{\kappa_2+\lambda_2}{2} \sinh(2h_2s)][(1-\lambda_1)h_1s - \frac{\kappa_1+\lambda_1}{2} \sinh(2h_1s)]. \quad (A.6)$$

APPENDIX B

The expressions for the functions K_{ij} , ($i, j = 1, 2$) which appear in (20):

$$K_{11}(x_1, t, s) = \frac{e^{-h_1 s}}{Q_3 Q_8 Q_9} \cosh(x_1 s) \{ \{ (3-2h_1 s - (2h_1 s + 3)e^{-2s(h_1+h_2)}) Q_3 - \alpha_1 Q_1 Q_5 \} \{ (2\alpha_2 s(h_1-t) - \alpha_2 + e^{-2h_1 s}) Q_3 + (1-\alpha_1 \alpha_2) Q_5 \} - Q_9 \{ (1+\alpha_1) Q_6 + 1 + e^{-2h_2 s} - 2(h_1-t) s e^{-2h_2 s} \} \} + \frac{2x_1 s}{Q_9} e^{-h_1 s} \sinh(x_1 s) [Q_3 \{ e^{-2h_1 s} - \alpha_2 + 2\alpha_2 s(h_1-t) \} + (1-\alpha_1 \alpha_2) Q_5],$$

$$K_{12}(x_1, t, s) = \frac{1+\alpha_2}{Q_3 Q_8 Q_9} e^{-h_1 s} \cosh(x_1 s) \{ \{ Q_3 (3-2h_1 s - (3+2h_1 s)e^{-2s(h_1+h_2)}) - \alpha_1 Q_1 Q_5 \} \{ Q_5 (2\alpha_4 s(h_2-t) - \alpha_4 + e^{-2h_2 s}) + Q_3 \} - \frac{1+\alpha_1}{1+\alpha_2} Q_9 \{ 4h_2 s e^{-4h_2 s} + (1-e^{-4h_2 s})(2sh_2 - 2st - 1) \} \} + \frac{1+\alpha_2}{Q_9} 2x_1 s e^{-h_1 s} \sinh(x_1 s) \{ Q_5 [2\alpha_4 s(h_2-t) - \alpha_4 + e^{-2h_2 s}] + Q_3 \},$$

$$K_{21}(x_2, t, s) = \frac{1+\alpha_4}{Q_4 Q_8 Q_9} e^{-h_2 s} \cosh(x_2 s) \{ \{ Q_4 (3-2h_2 s - (3+2h_2 s)e^{-2s(h_1+h_2)}) + \alpha_3 Q_2 Q_5 \} \{ Q_5 (\alpha_2 - 2\alpha_2 s(h_1-t) - e^{-2h_1 s}) + Q_4 \} - \frac{1+\alpha_3}{1+\alpha_4} Q_9 \{ 4h_1 s e^{-4h_1 s} + (1-e^{-4h_1 s})(2h_1 s - 2ts - 1) \} \} + \frac{1+\alpha_4}{Q_9} 2s x_2 e^{-h_2 s} \sinh(x_2 s) [Q_5 (\alpha_2 - 2\alpha_2 s(h_1-t) - e^{-2h_1 s}) + Q_4],$$

$$K_{22}(x_2, t, s) = \frac{e^{-h_2 s}}{Q_4 Q_8 Q_9} \cosh(x_2 s) \{ \{ Q_4 (3-2h_2 s - (3+2h_2 s)e^{-2s(h_1+h_2)}) + \alpha_3 Q_2 Q_5 \} \{ Q_4 (2\alpha_4 s(h_2-t) - \alpha_4 + e^{-2h_2 s}) + (\alpha_3 \alpha_4 - 1) Q_5 \} \}$$

$$\begin{aligned}
& - Q_9 \{ 1 + e^{-2h_2 s} - 2s(h_2 - t)e^{-2h_1 s} + (1 + \alpha_3)Q_7 \}] \\
& + \frac{2sx_2}{Q_9} e^{-h_2 s} \sinh(x_2 s) [Q_4 (2\alpha_4 s(h_2 - t) - \alpha_4 + e^{-2h_2 s}) \\
& - (1 - \alpha_3 \alpha_4)Q_5], \quad (B.1a-d)
\end{aligned}$$

where

$$\begin{aligned}
\alpha_1 &= (\kappa_1 \mu_2 - \kappa_2 \mu_1) / (\mu_2 + \kappa_2 \mu_1), \quad \alpha_2 = (\mu_2 - \mu_1) / (\mu_1 + \kappa_1 \mu_2), \\
\alpha_3 &= (\kappa_2 \mu_1 - \kappa_1 \mu_2) / (\mu_1 + \kappa_1 \mu_2), \quad \alpha_4 = (\mu_1 - \mu_2) / (\mu_2 + \kappa_2 \mu_1), \quad (B.2) \\
Q_1 &= \frac{4h_2 s}{\alpha_3} e^{-2h_2 s} - 1 + e^{-4h_2 s}, \quad Q_2 = \frac{4h_1 s}{\alpha_1} e^{-2h_1 s} - 1 + e^{-4h_1 s}, \\
Q_3 &= e^{-4h_2 s} + 4\alpha_4 s h_2 e^{-2h_2 s} - 1, \quad Q_4 = e^{-4h_1 s} + 4\alpha_2 s h_1 e^{-2h_1 s} - 1, \\
Q_5 &= e^{-2h_1 s} - e^{-2h_2 s}, \quad Q_6 = 1 + 4s h_2 e^{-2s h_2} - e^{-4s h_2}, \\
Q_7 &= 1 + 4h_1 s e^{-2h_1 s} - e^{-4h_1 s}, \quad Q_8 = 1 - e^{-2s(h_1 + h_2)}, \\
Q_9 &= (\alpha_1 \alpha_2 - 1)Q_5^2 + Q_3 Q_4. \quad (B.3)
\end{aligned}$$

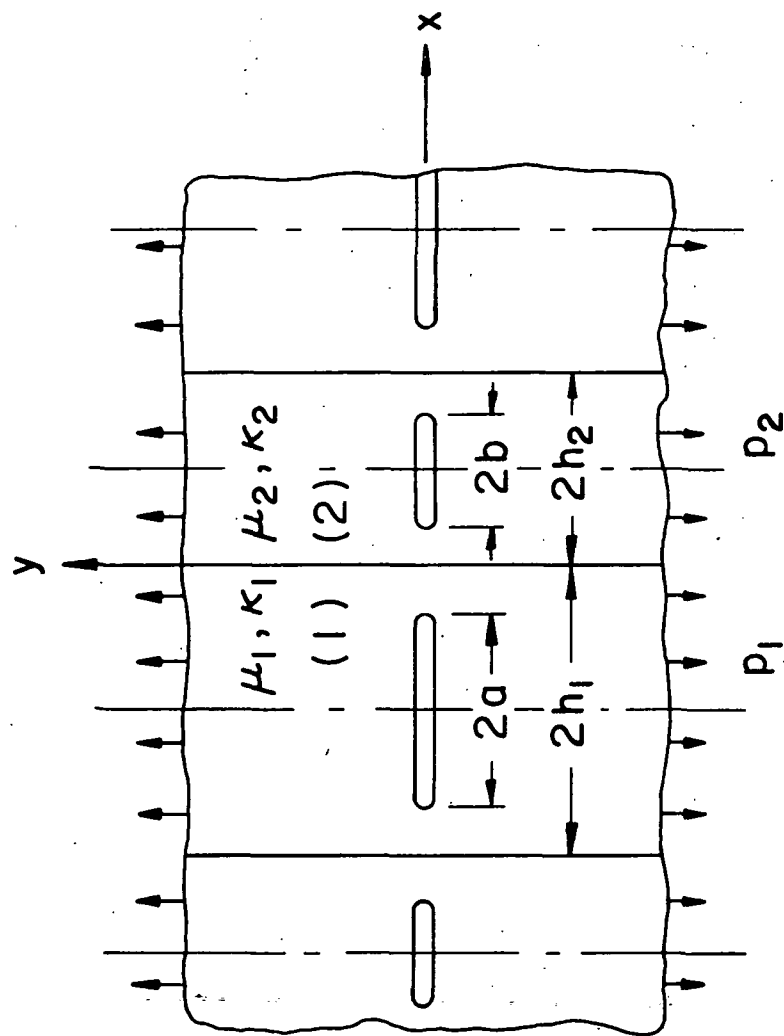


Figure 1. Geometry of the composite plate.

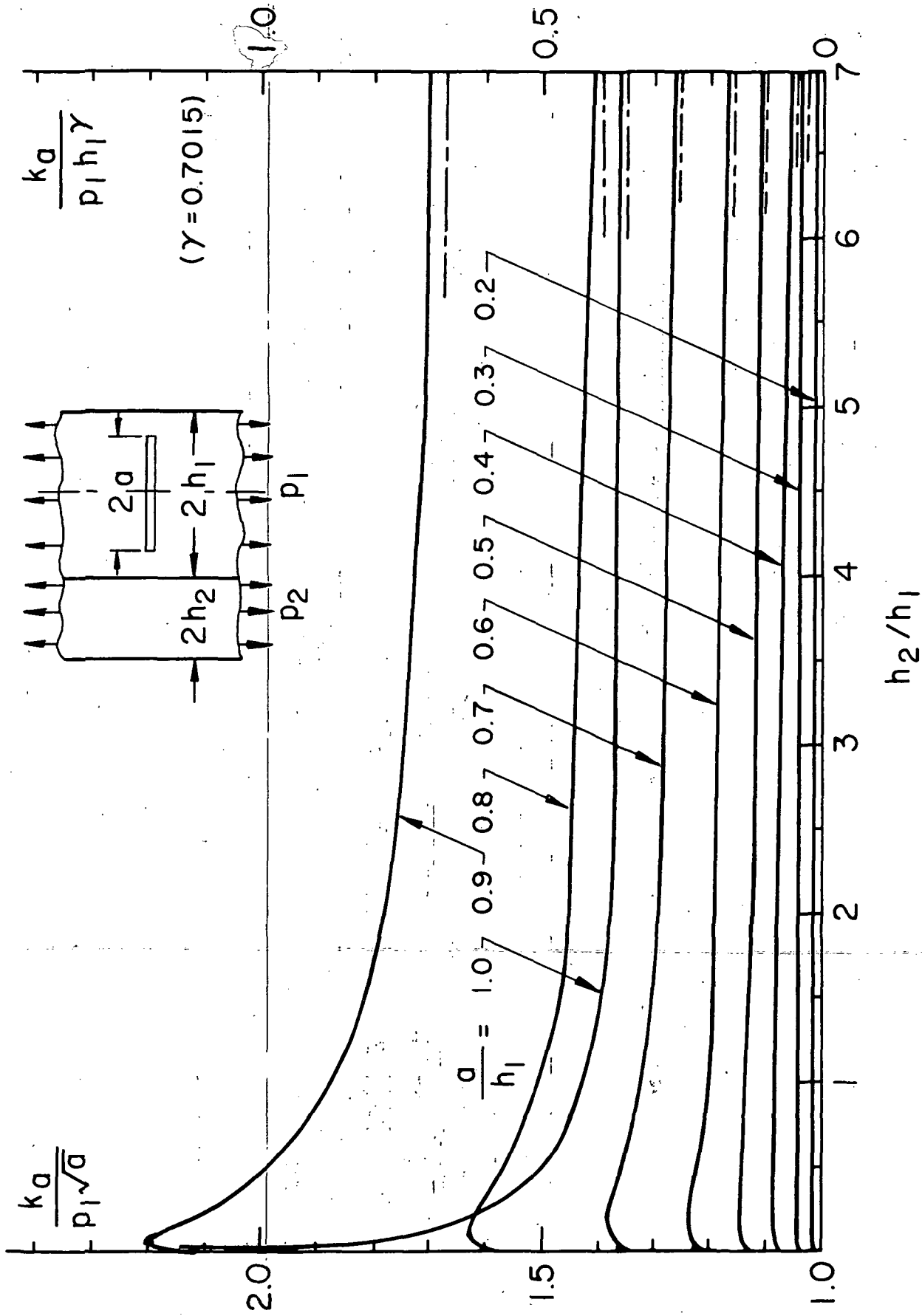


Figure 2.

The stress intensity factor k_a for the crack
 in stiff material ($b = 0$, $\mu_1 = 6.65\mu_2$, $\nu_1 = 0.35$,
 $\nu_2 = 0.45$; the scale on the right corresponds to
 $a = h_1$ curve).

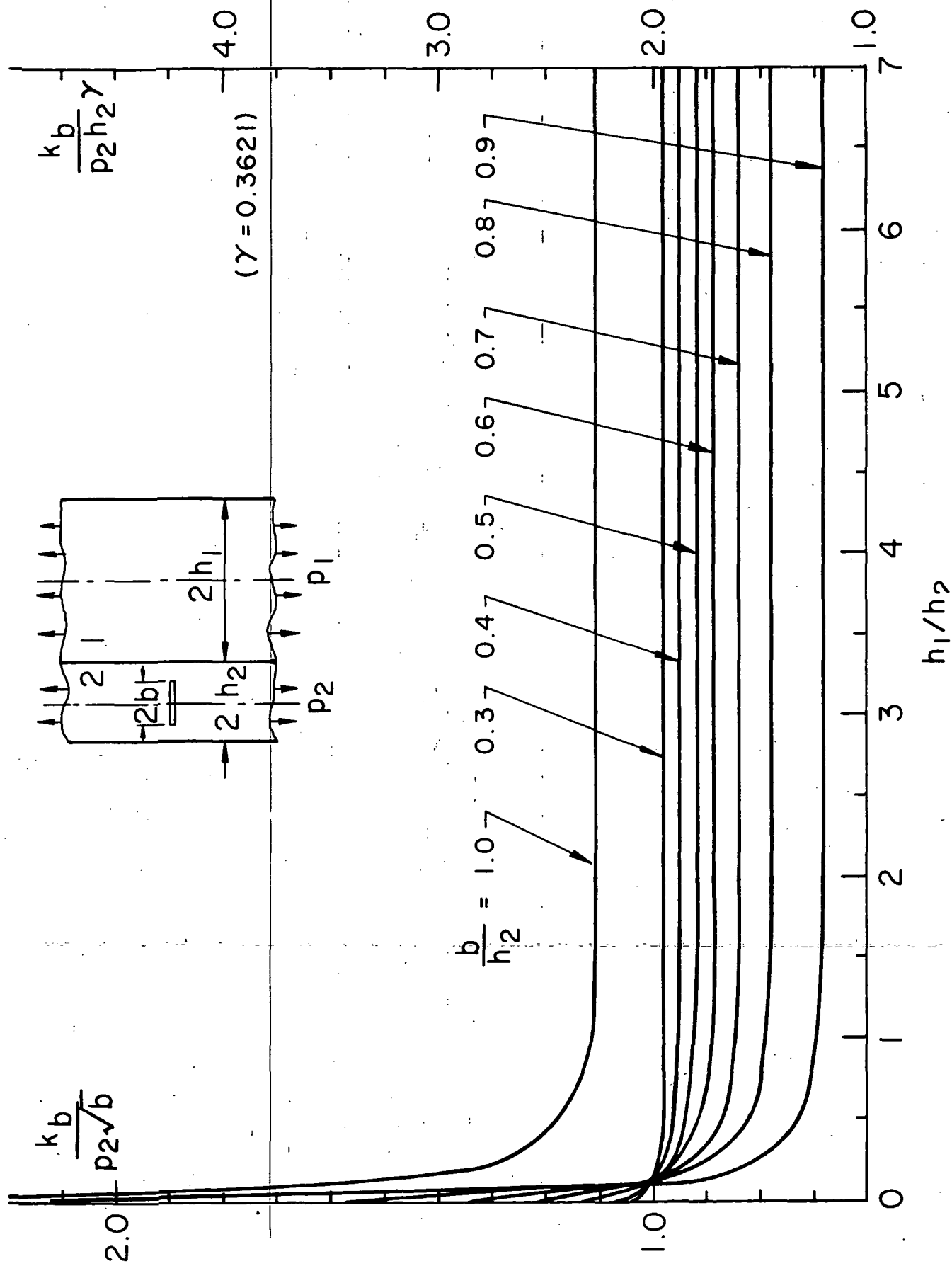


Figure 3. The stress intensity factor k_b for the crack in buffer strip ($a = 0$; $b \leq h_2$; the scale on the right corresponds to $b = h_2$ curve).

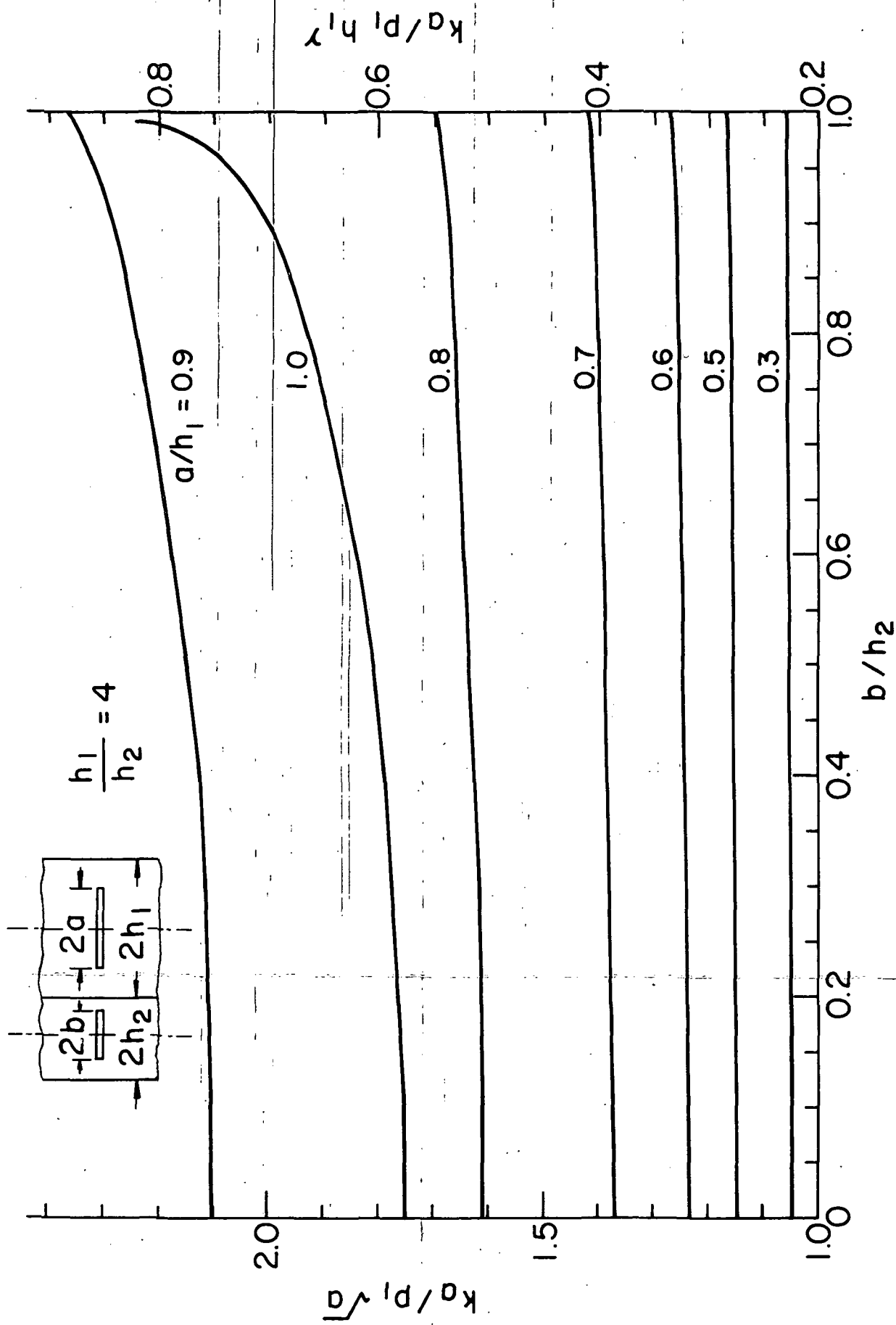


Figure 4.

The stress intensity factor k_a for the case in which both strips contain cracks ($h_1 = 4h_2$, $\mu_1 = 6.65\mu_2$, $\nu_1 = 0.35$, $\nu_2 = 0.45$; the scale on the right corresponds to $a = h_1$ curve).

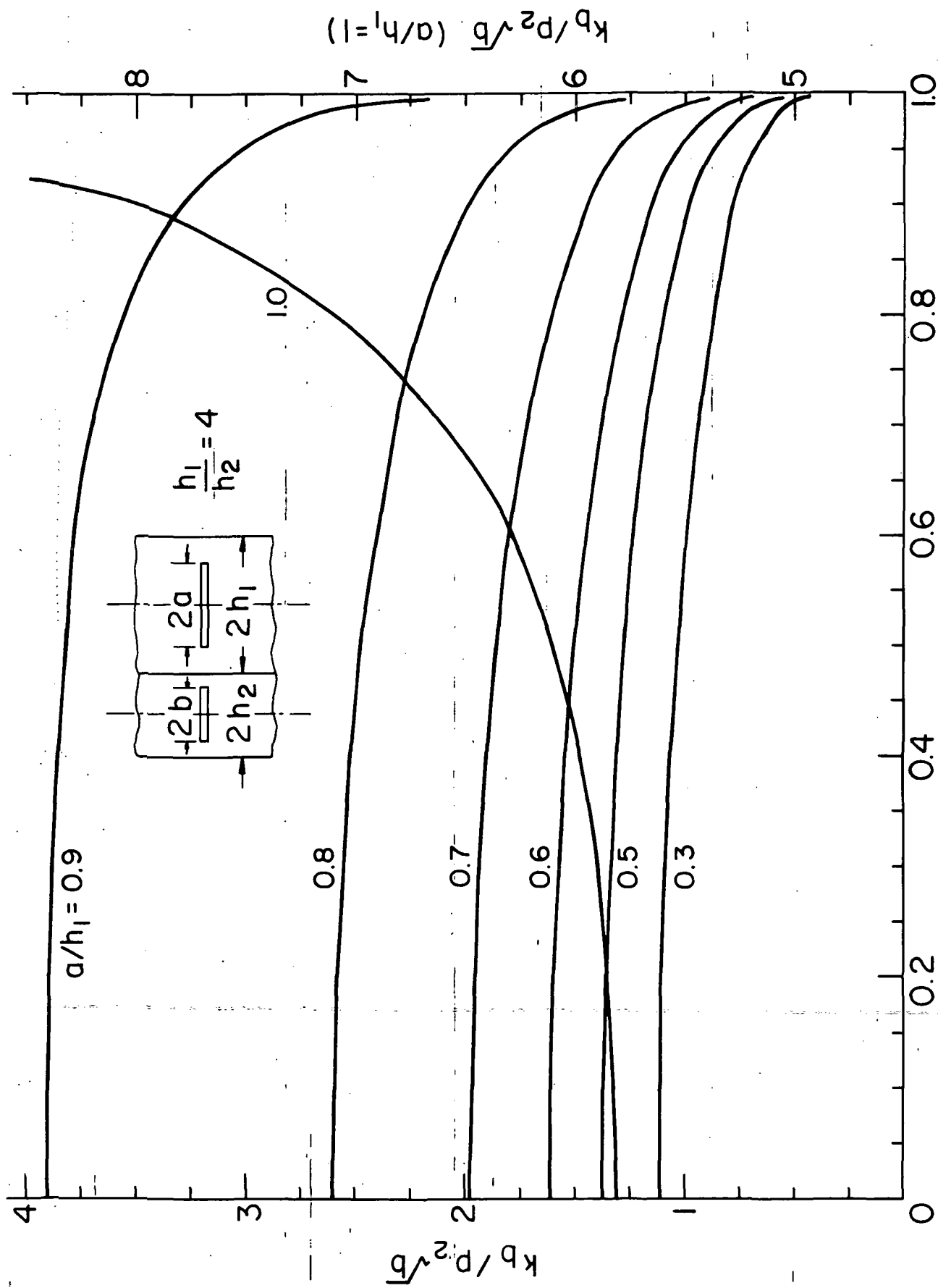


Figure 5. The stress intensity factor k_b for the case in which both strips contain cracks ($h_1 = 4h_2$, $\mu_1 = 6.65\mu_2$, $\nu_1 = 0.35$, $\nu_2 = 0.45$; the scale on the right corresponds to $a = h_1$ curve).